

Detailed kinetics of soot formation from aromatic fuels pyrolysis

T. Viola¹, L. Carneiro Piton¹, A. Nobili², M. Idir¹, S. Abid¹, N. Chaumeix¹, A. Comandini¹

¹Institut de Combustion, Aérothermique, Réactivité et Environnement, CNRS-INSIS UPR-3021, Orléans, France

²Department of Chemistry, Materials, and Chemical Engineering, Politecnico di Milano, Italy

Abstract

Understanding soot formation is a key factor for the development of next-generation clean combustion devices. In this paper, a new detailed mechanism for soot formation under pyrolytic conditions is presented. The work has been performed at ICARE – CNRS through the implementation of a python framework for automated mechanism generation (SMAuG - Soot Mechanism Automated Generator) which allowed the development of the solid-phase chemistry model. Such model is combined with the gas-phase mechanism developed in previous works specifically focused on PAH chemistry in single-pulse shock tube experiments, up to C18 products. In addition, the polyynes chemistry has also been added through an upgrade of the gas phase kinetics part from literature up to C12 and the implementation of the reactions of polyynes in the soot model from inception in combination with PAHs and then surface growth. Initial comparisons of the new combined mechanism were made against experimental data, mainly soot volume fractions, from toluene pyrolysis obtained at ICARE by shock tube techniques.

1 Introduction

The formation of carbonaceous soot particles is a complex mechanism which involves several multi-steps, multi-phase chemical and physical processes [1,2]. This complexity poses serious limitations to our capability to accurately model soot emissions from combustion devices, as accurately as needed for the development of solutions for next generation clean combustion technologies (engine optimization and fuel re-formulation). Detailed chemical kinetic soot models have been developed in the past based on laboratory-based experimental results. Among such models, sectional models have been popular for several years as they offer the possibility of building “apparently simplified” models for complex phenomenology such as soot formation in combustion, thanks to the use of lumped chemical species and reactions. The mechanism presented in this paper is the first version of ICARE_SMAuG_v1, which combines the gas-phase PAH chemistry from our previous works [3] with the new solid-phase chemistry mechanism. Such mechanism is generated through the implementation of SMAuG (Soot Mechanism

Correspondence to: andrea.comandini@cnrs-orleans.fr

Automated Generator) framework in python currently calibrated on the automated generation of detailed kinetic mechanisms of soot formation in pyrolytic conditions. 12 classes of reactions considered fundamental for soot nucleation and growth were considered. In addition, the gas-phase chemistry of ICARE_SMAuG_v1 model includes updated reactions for the pathway of polyynes as described in literature [4] and in particular using values from [5,6]. Experimental results on toluene pyrolysis were also obtained using conventional shock tube laser-based techniques, for validation of the current model.

2 Experimental Setup and SMAuG

In order to evaluate an initial performance of the proposed mechanism, the key features of which are outlined below, the heated shock tube (HST) at ICARE was implemented to obtain experimental results on toluene pyrolysis. The set-up is briefly described here. The HST is a widely used shock tube at ICARE for high-temperature chemical kinetics, in particular on soot formation [7,8]. In total it has a length of $L=7.15$ m, a 52.4 mm diameter driven section and a 114.3 mm diameter driver section made entirely of stainless steel, capable of operating at a maximum pressure of 60 bar. It is equipped with four pressure sensors (CHIMIE METAL A25L05B) positioned along the shock tube at a distance of 150 mm from each other. The sensors are used to measure the incident shock wave velocity extrapolated to the end-wall, from which the thermodynamic conditions behind the reflected shock waves can be calculated by solving the conservation equations. The computed T_5 has a maximum error of 25-30 K due to the wave attenuation and the uncertainty in determining the exact positions of the pressure sensor sensitive surfaces. A PCB Piezotronics pressure sensor located at the end-wall of the driven section measures the pressure-time profiles. The signal acquisition is obtained with three Rohde&Schwartz RTB 2004 oscilloscopes that record pressure signals and signals from the laser acquisition system. Two lasers are used for quantification and characterization of the produced soot. Extinction measurements for quantification of soot volume fractions are carried out with a He:Ne laser @ $\lambda=633$ nm, while extinction/Rayleigh scattering measurements with a Nd:Yag laser @ $\lambda=532$ nm are implemented for the determination of the particle size. The detectors, both at 532nm and 633nm, are HAMAMATSU R59838 photomultiplier tubes. For ICARE_SMAuG_v1 comparisons, the soot volume fractions f_v 's at 2 ms and 4 ms are calculated as in equation (1), where m is the complex refractive index of soot particles, l the length crossed by the incident beam (diameter of the shock tube), λ the wavelength of the transmitted beam, I_0 the intensity of the incident beam. The function of the refractive index is assumed to be 0.36 as used in previous works in the literature, e.g. [9,10]. The experiments were performed with 0.07% toluene in argon, pressure behind the reflected shock wave between 16 and 18 bar, and initial carbon concentrations of $3-4 \times 10^{17}$ atoms/cm³.

$$f_v = \frac{\lambda}{6\pi l \operatorname{Im}\left(\frac{m^2-1}{m^2+1}\right)} \ln \frac{I}{I_0} \quad \text{Eqn. 1 Experimental evaluation of soot volume fraction } f_v.$$

Regarding the ICARE_Smaug_v1, it is basically modeled on the concept of pseudo lumped species BINs and its sections are implemented on the line of the scheme of the recent CRECK mechanism [11]. The framework is characterized by several .csv files containing the input information, including the reactant chemical species for the different classes (radicals, resonantly stabilized radicals, molecules, BINs). The kinetic parameters of the reference reaction for a specific class of reactions, at present, can be entered through a dual system i.e., from the launcher or from the .csv files themselves where the species are declared. The parameters are then scaled based on chemical kinetic theory. In particular, the BINs-BINs interactions from inception to aggregation are scaled according to [12]. The reference kinetic parameters are reported in Table 1. SMAuG's dedicated launcher allows it to interact with its core to use chemical species, kinetic parameters and reactions in order to generate kinetics and thermodynamics files in .dat, .CKI and .CKT, .cti and .yaml.

				Ref.
ICARE – Gas phase up to C18				[3]
Polyynes C₂NH₂ radicals (PYYNr) and molecules (PYYNm) up to C12				[5]
SMAuG v1 Soot model reaction classes				
	A	n	Ea	
HACA				
H-abstraction				
H + BINi → H ₂ + BINj (i ≤ 3)	4.8·10E+6	2	10500	[11]
Acetylene addition				
C ₂ H ₂ + BINj → products (i ≤ 3)	1.0·10E+12	0	5000	-
C ₂ H ₂ + BINj → products (i > 3)	1.0·10E+12	0	10000	-
Soot Inception				
Small Resonantly Stabilized Radicals+PAHs				
SRSR + PAHr	3.0·10E+12	0.5	0	[this work]
Polyynes + PAHs				
PYYNr + PAHr	1.0·10E+13	0	0	-
PYYNr + PAHm	1.0·10E+13	0	8000	-
PYYNm + PAHr	1.0·10E+13	0	8000	-
PYYNm + PAHm	1.2·10E+12	0	8000	-
PAHs + PAHs				
PAHr + PAHr	5.0·10E+10	0.5	0	[this work]
PAHr + PAHm	5.0·10E+10	0.5	8000	-
PAHrsr + PAHr	2.0·10E+12	0	3000	-
PAHrsr + PAHm	5.0·10E+12	0	17000	-
PAHrsr + PAHrsr	4.0·10E+12	0	5500	-
PAHm + PAHm	1.2·10E+9	0.5	0	-
PAHs + BINs				
PAHr + BINj	1.2·10E+13	0	0	[this work]
PAHm + BINj	1.2·10E+13	0	6000	-
PAHr + BINi	1.0·10E+13	0	6000	-
BIN/BINJ				
BINj + BINn → products (i ≤ 4 and n ≤ 5)	1.6·10E+13	0.5	0/5000	[this work]
BINi + BINn → products (i ≤ 3 and n ≤ 5)	1.6·10E+13	0.5	6670	-
BINi + BINn → products (i ≤ 2 and n ≤ 3)	1.6·10E+12	0.5	6670	-
Surface growth				
SRSR + BINj → products (i ≤ 3)	2.5·10E+13	0	5000	[11]
SRSR + BINj → products	2.0·10E+12	0	19000	-
PYYNr + BINj → products	4.0·10E+13	0	0	[6]
PYYNm + BINj → products	4.0·10E+13	0	0	-
PAHm + BINj → products (i ≤ 3)	4.0·10E+13	0	8000	[11]
PAHm + BINj → products (i > 3)	5.0·10E+14	0.5	23000	-
PAHrsr + BINj → products (i ≤ 3)	4.0·10E+13	0.5	11500	[this work]
PAHr + BINj → products (i ≤ 3)	4.0·10E+13	0	0/3000	-
PAHr + BINj → products (i > 3)	5.0·10E+14	0.5	23500	[11]
BINi + BINn → products (i ≤ 3 and n ≥ 5)	1.6·10E+13	0.5	0	-
Dehydrogenation				
Dehydrogenation				
BINj → H ₂ + BINj	1.0·10E+8	0	32000	[11]
BINj → H· + BINi (i ≤ 3)	1.0·10E+11	0	12000	-
Demethylation				
H· + BINj → CH ₃ · + products	1.2·10E+13	0	5000	-
C-H fission/recombination				
BINi → H· + BINj (i ≤ 3)	1.5·10E+17	0	114000	-
H· + BINj → BINi (i ≤ 3)	1.0·10E+14	0	0	-
Particle coalescence & Aggregation				
BINi· + BINn· → products (i, n ≥ 5)	1.6·10E+13	0.5	0	[11]

The units of the kinetic rate parameters are in K, L, s, cal

Table 1. ICARE_SMAuG_v1 Sections, reactions and rate kinetic parameters.

3 Results and discussion

The mechanism currently generated by SMAuG and coupled with ICARE gas phase includes 644 chemical species and 17326 reactions. At the current state of version 1.0 of SMAuG, it is possible to run 0D simulations with a batch isothermal and constant pressure reactor defined on Cantera [13] to postprocess the results and calculate the soot volume fractions using Eqn.2:

$$f_{v_model} = \frac{\rho}{\rho_{soot}} \sum_{i=5}^{25} w_i$$

Eqn. 2 f_{v_model} soot volume fraction implemented for SMAuG.

In eqn.2 ρ is the density of the gas, ρ_{soot} a general averaged estimated value of soot density, in this work 1800 kg/m^3 , and w_i are the mass fractions of the BINs produced (from 5 to 25) considering a range of a ESD in nm from 2 to 202.

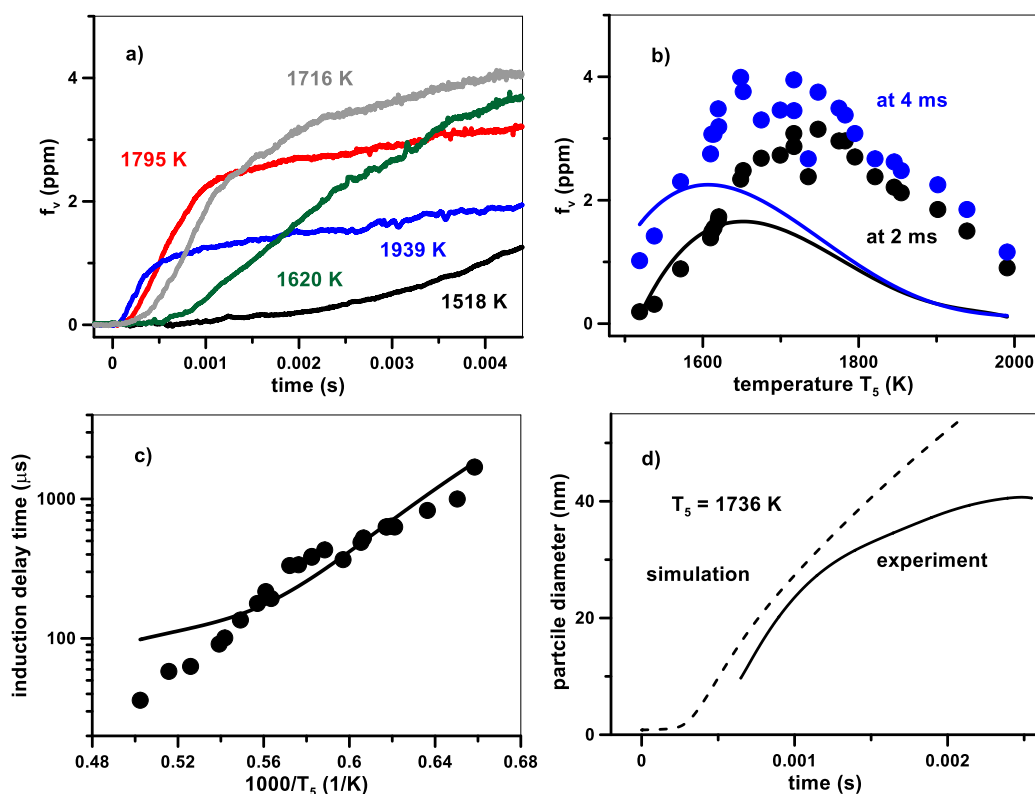


Figure 1. Experiments and simulations of 0.07% toluene in argon.

Figure 1 provides an enhanced view of the predictivity of the mechanism for the experimental data set obtained in the present work (0.07% C_7H_8 in argon). Figure 1a contains examples of soot volume fraction time-history profiles at different temperature conditions. As expected based on common features of soot profiles in shock tube experiments, the soot starts forming earlier at higher temperatures, while the maximum soot volume fraction is attained at around 1720 K before decreasing at higher temperatures. The profiles can be used to derive several kinetic parameters. First, the soot volume fractions at fixed times (2 and 4 ms) are reported in Figure 1b, together with the modeling results. As mentioned above, the maximum is reached at temperatures between 1700 and 1750 K. The kinetic model

shows trends which are shifted towards lower temperatures, which results in an underprediction of the soot volume fractions at high temperature conditions. On the other hand, the simulations show that the curves at 2 and 4 ms converge at higher temperatures, as in the experiments. Concerning the induction delay times, defined as the time between the arrival of the shock wave at the endwall and the time obtained extrapolating the maximum slope of the f_v curve to the baseline, the model provides a good description of the experimental curve at lower temperatures, while an overprediction of the induction delay times is observed at higher temperature conditions (Figure 1c). Finally, the average particle diameter as measured by Rayleigh scattering is presented in Figure 1d for an experiment at $T_5 = 1736$ K. The simulation profile is slightly shifted towards earlier times, but the overall trend is reproduced. At present, further relevant fine-tuning of kinetic parameters is needed to develop other versions of the mechanism that can make better and more accurate predictions in relation with the most significant discrepancies from the experimental data, especially at high temperatures. In order to achieve this, simulations and comparisons with experimental data from the HST will be carried out for different fuel molecules and mixtures. Therefore, the parameters presented in Table 1 should only be considered as a first attempt to set up the reaction mechanism that will require further implementations. In the meantime, SMAuG will be further developed with analysis tools and optimized for soot model generation.

Acknowledgements

This project has received funding from the European Research Council (ERC) under the European Union's Horizon 2020 research and innovation programme (grant agreement No. 756785).

References

- [1] Bockhorn, H. A Short Introduction to the Problem. In *Soot Formation in Combustion-Mechanisms and Models*, Bockhorn H., Ed.; Springer Series in Chemical Physics, Volume 59, 1994, pp 3-9.
- [2] Lighty, J. S.; Veranth, J. M.; Sarofim, A. F. Combustion aerosols: factors governing their size and composition and implications to human health. *J. Air Waste Manage.* 2000, 50, 1565-1618.
- [3] Sun, W., Hamadi, A., Abid, S., Chaumeix, N., Comandini, A., 2021. Influences of propylene/propyne addition on toluene pyrolysis in a single-pulse shock tube. *Combustion and Flame* 236. <https://doi.org/10.1016/j.combustflame.2021.111799>;
- [4] Krestinin, A.V., 1998. Polyne model of soot formation process. Symposium (International) on Combustion, Twenty-Seventh Symposium (International) on Combustion Volume One 27, 1557–1563. [https://doi.org/10.1016/S0082-0784\(98\)80564-X](https://doi.org/10.1016/S0082-0784(98)80564-X);
- [5] Zhil'tsova, I.V., Zaslanko, I.S., Karasevich, Yu.K., Wagner, H.Gg., 2000. Nonisothermal effects in the process of soot formation in ethylene pyrolysis behind shock waves. *Kinet Catal* 41, 76–89. <https://doi.org/10.1007/BF02756145>;
- [6] Wen, J.Z., Thomson, M.J., Lightstone, M.F., Rogak, S.N., 2006. Detailed Kinetic Modeling of Carbonaceous Nanoparticle Inception and Surface Growth during the Pyrolysis of C₆H₆ behind Shock Waves. *Energy Fuels* 20, 547–559. <https://doi.org/10.1021/ef050081q>;
- [7] De Iuliis, S., Chaumeix, N., Idir, M., Paillard, C.-E., 2008. Scattering/extinction measurements of soot formation in a shock tube. *Experimental Thermal and Fluid Science*, Fifth mediterranean combustion symposium 32, 1354–1362. <https://doi.org/10.1016/j.expthermflusci.2007.11.008>;
- [8] Mathieu, O., Djebaili-Chaumeix, N., Paillard, C.-E., Douce, F., 2009. Experimental study of soot formation from a diesel fuel surrogate in a shock tube. *Combustion and Flame* 156, 1576–1586. <https://doi.org/10.1016/j.combustflame.2009.05.002>;
- [9] Agafonov, G. L.; Biler, I. V.; Vlasov, P. A.; Kolbanovskii, Y. A.; Smirnov, V. N.; Tereza, A. M., Soot formation during the pyrolysis and oxidation of acetylene and ethylene in shock waves. *Kinet. Catal.* 2015, 56, 12-30.

- [10] Nativel, D.; Herzler, J.; Krzywdziak, S.; Peukert, S.; Fikri, M.; Schulz, C., Shock-tube study of the influence of oxygenated additives on benzene pyrolysis: Measurement of optical densities, soot inception times and comparison with simulations. *Combust. Flame* 2022, 111985
- [11] Nobili, A., Cuoci, A., Pejpichestakul, W., Pelucchi, M., Cavallotti, C., Faravelli, T., 2022. Modeling soot particles as stable radicals: a chemical kinetic study on formation and oxidation. Part I. Soot formation in ethylene laminar premixed and counterflow diffusion flames. *Combustion and Flame* 112073. <https://doi.org/10.1016/j.combustflame.2022.112073>
- [12] A. D'Alessio; A. Barone; R. Cau; A. D'Anna; P. Minutolo, *Proceedings of the Combustion Institute* 30 (2005) 2595-2603.
- [13] Cantera is an open-source suite of tools for problems involving chemical kinetics, thermodynamics, and transport processes. <https://cantera.org/> .